DOI: 10.1002/cphc. 200((will be filled in by the editorial staff))

Modification of electrode surfaces by self-assembled monolayers of thiol-terminated oligo(phenyleneethynylene)s

Inderpreet Kaur,[a] Xiaotao Zhao,[b] Martin R. Bryce,[b] Phil A. Schauer,[b] Paul J. Low[b] and Ritu Kataky*[b]

*The wire-like properties of four S,-[4-[2-[4-(2-phenylethynyl)phenyl]ethynyl]phenyl]thioacetate derivatives, PhC≡CC$_6$H$_4$C≡CC$_6$H$_4$SAc **1,** H$_2$NC$_6$H$_4$C≡CC$_6$H$_4$C≡CC$_6$H$_4$SAc **2,** PhC≡CC$_6$H$_2$(OMe)$_2$C≡CC$_6$H$_4$SAc **3** and AcSC$_6$H$_4$C≡CC$_6$H$_4$C≡CC$_6$H$_4$SAc **4 (Figure 1)**, all of which possess a high degree of conjugation along the oligo(phenyleneethynylene) (OPE) backbone, were investigated as self-assembled monolayers (SAMs) on gold and platinum electrodes by cyclic voltammetry (CV) and electrochemical impedance spectroscopy (EIS). The redox probe [Fe(CN)$_6$]$^{4-}$ was used in both the CV and impedance experiments. The results indicate that the thiolates derived from thioacetate-protected precursor molecules **1** and **2** form well-ordered monolayers on a gold electrode, whereas SAMs derived from **3** and **4** exhibit randomly distributed pinholes. The electron tunnelling resistance and fractional coverage of self-assembled monolayers (SAMs) of all four compounds were examined using electron tunnelling theory. The analysis of the results revealed that the well-ordered SAMs of **1** and **2** exhibit higher charge transfer resistance in comparison to the defect-ridden SAMs of **3** and **4**. The addition steric bulk offered by the methoxy groups in **3** likely prevent efficient packing within the SAM, leading to microelectrode behaviour, when assembled on a gold electrode surface. The protected dithiol derivative **4** probably binds to the surface through both terminal groups which prevents dense packing and leads to the formation of a monolayer with randomly distributed pinholes. Atomic force microscopy (AFM) was used to examine the morphology of the monolayers and height images gave root-mean-square (RMS) roughness's which are in agreement with the proposed SAM structures.*

Introduction

Self-assembled monolayers (SAMs) have received much attention due to their potential applications in nanotechnology, for molecular recognition and fabrication of various nanodevices such as sensors,[1-7] biosensors,[8-13] actuators[14-15] ,molecular motors[16] and photochromic devices. Other important applications of SAMs include use in the fabrication of corrosion resistive coatings,[17-19] as active or passive elements in electronic devices,[20-22] and as inks in dip pen lithography.[23-26] Additionally, SAMs can serve as models to study the properties of membranes in cell organelles, and can be used as building blocks for biomimetic systems. Self-assembly of organic molecules on a solid surface provides an interface which connects two worlds of entirely different physical and chemical properties, for example a metal on one side and an organic domain on other side. SAMs of alkanethiols and alkanedithiols on gold [27-43] are the most extensively studied due to the formation of well packed structures with relatively high stability, which can suppress supress electrochemical processes directly at the metal-solution interface. SAMs have, additionally, been prepared by chemisorption of organic molecules containing various functional groups such as -SH,[28] -COOH,[29] -NH_2,[30,31] etc. and are also known on a variety of electrode surfaces other than gold, such as platinum,[31,44-46] copper,[47-48] silver[49] and silicon.[50-51]

Although well-ordered and defect free SAMs are often an idealised target structure, self-assembled monolayers may contain pinholes or defects which would restrict use in many applications. Porter *et al.*[52] reported SAMs of long-chain alkanethiols through to be pinhole-free on the basis of cyclic voltammetric studies. On the other hand, Finklea[53] and Sabatani[54] suggested that gold electrodes modified by long alkyl SAMs may exhibit electron transfer at pinholes and electron tunnelling at defects, which was demonstrated using impedance studies. Different research groups have emphasized that the quality, stability and compactness of the SAM predominantly depend not only on the physical and chemical structure of the constituent molecules and the nature of the molecule-surface interaction, but also upon the cleanliness of the electrode surface and mode of preparation. However, self-assembled monolayers of thiols on gold hold a privileged position within the field of single-molecule electronics and studies of the electrical behaviour of thiol-based SAMs on gold have been of immeasurable importance in assessing the wire-like properties of various molecular backbones in metal/molecule/metal junctions. [55]

Each molecule used in the fabrication of SAMs in this work, consists of three parts: (a) a head group which can bond with the metal electrodes of choice, namely gold and platinum, (b) a conjugated hydrocarbon backbone which stabilizes the SAM through intermolecular Van der Waals interactions, and (c) a functional tail group that provides interaction to the second interface and which can in principle be tailored by further chemical modification.[41] This work explores the self-assembly properties of four wire-like *S*,-[4-[2-[4-(2- phenylethynyl)phenyl]-ethynyl]phenyl] thioacetate derivatives **1, 2, 3** and **4 (Figure 1)** on gold and platinum electrodes and offers and analysis of the homogeneity and structure of the resulting monolayers using CV and electrochemical impedance spectroscopy data.

[a] *Dr. Inderpreet Kaur,*
Department of Chemistry,
Guru Nanak Dev University, Amritsar, INDIA
E-mail address: inderpreet11@yahoo.co.in

[b] *Dr. Ritu Kataky, Xiaotao Zhao, Prof. Martin R. Bryce,*
Phil A. Schauer, Prof. Paul J. Low,
Department of Chemistry, Durham University,
Durham, DH1 3LE, United Kingdom
E-mail address: ritu.kataky@durham.ac.uk

These linear π-conjugated molecular wires are length persistent rigid rodlike molecules although low energy rotation can occur around the phenyl-ethynyl bonds in the backbone, in fluid media and the gas phase,[56,57] but cannot fold or undergo *cis-trans* isomerism which complicates the study of oligo(phenylenevinylene) (OPV) analogues. The thioacetate terminated molecules **1-4** studied here bind to the gold surface via thiolate units which are formed during deposition.[43] The structural variants were chosen to probe the effects of different end groups (-H, -NH_2 or -SR) and the steric effect of dimethoxy substitution in the central ring (derivative **3**) while retaining the same backbone structure.[57] Rigid linear molecules such as **1-4** bearing two terminal end-groups that are both capable of coordination with metal surface can align approximately normal to the surface through coordination of one or other of the surface binding groups, or lie closer to parrallel to the surface with both groups binding to the surface.[59] Thiol-amine and thiol-thiol competition for the binding to the gold surface may be expected in SAMs formed from molecules **2** and **4,** respectively and it is not possible from simple inspection of the molecular structure to predict the formation of a homogeneously ordered SAM. While Rosario-Castro performed the electrochemical and surface characterization of self-assembled monolayer of 4-aminothiophenol (4-ATP) at platinum electrode and reported that the molecules of 4-ATP are sulfur-bonded to the platinum surfaces which lead to the formation of an amino-terminated electrode surface,[31] on gold this molecule tends to give more complex heterogeneously structured films.[59] Langmuir-Blodgett (LB) methods provide an alternative route to the formation of well-ordered molecular films, and LB films of **2** on gold in both Au-S and Au-N orientations and the electronic characteristics described, recently.[58] The present work highlights the self-assembly of the four, bifunctional molecular wire candidates **1** - **5** on Au and Pt surfaces.

Cyclic voltammetry (CV) was applied to investigate the degree of order and compactness of the SAMs formed from **1** - **4** under conditions known to result in removal of the protecting group.[43] The results of CV and impedance studies have shown that the thioacetate-protected precursors **1** and **2** form well-behaved monolayers on a gold electrode in comparison to SAMs formed from **3** and **4**, which exhibit randomly distributed pinholes and defects.

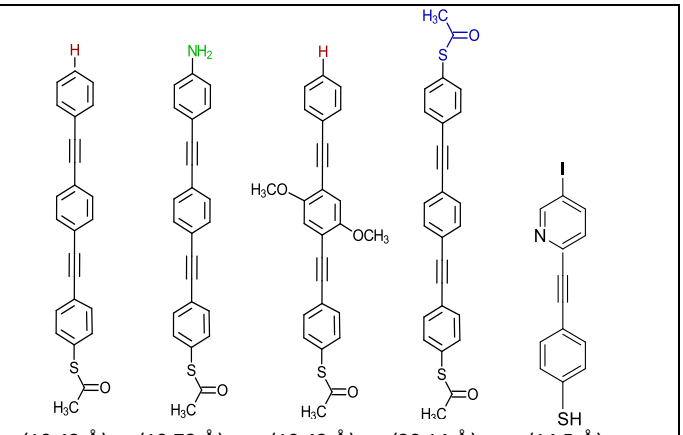

Figure 1. Structures of S,-[4-[2-[4-(2-phenylethynyl)phenyl] ethynyl] phenyl] thioacetate molecular wires **1**, **2**, **3** and **4** and their calculated molecular lengths S...C (**1** and **3),** S...N (**2**). And S...S (**4**) and S-Me (5). 5* is Oligo(aryleneethylene) 2 in reference 42.

The SAMs formed from each compound were imaged using atomic force microscopy (AFM) to examine the topographic surface and a section analysis of height images gave root-mean-square (RMS) roughness. In addition, the SAMs of all the four compounds were also investigated on a platinum electrode surface and the rates of electron transfer through the films on both substrates were evaluated. The results show **1** - **4** have high affinity towards self-assembly on gold, less so on platinum, with **1** and **2** giving the most densely packed and well-ordered films.

Results and Discussion

Electrochemical Studies

(A) Cyclic voltammetry

Cyclic voltammetry (CV) was used to investigate the degree and compactness of the SAMs of the four molecular wires **1, 2, 3** and **4** (Figure 2). In this work, $[Fe(CN)_6]^{3-}$ which shows a well-behaved electrochemically reversible, one-electron, outer-sphere redox couple, was used as a redox probe molecule. The CV experiments with modified electrodes were carried out in aqueous 1 mM $K_4Fe(CN)_6$ solution in 0.1 M KNO_3 for potential sweeps from -0.2V to +0.6V with the scan rate of 50 mV/s. In **Figure 2 (A) – (D) and (A') - (D')**, the broken line displays a typical CV response for the bare gold or platinum electrodes, as indicated by the shape of the voltammogram, showing the electron transfer across the interface controlled by mass transfer. The solid lines show CV responses for the gold and platinum electrodes covered with a monolayer of **1, 2, 3** or **4** and of **mixed monolayers of 3, and 4 +DDT.**

Monolayers on Gold Electrodes

It is clear from **Figure 2(A)** and **2(B)** that there is a significant difference in the CV responses of the bare gold electrodes and the gold electrodes covered with SAMs derived from **1** and **2.** The current is significantly reduced for **1 SAM** and **2 SAM** and the complete absence of peaks in the cyclic voltammograms indicate that the redox reaction is almost completely suppressed, albeit with the observation of small residual tunnelling currents. In previous work, [42] we have shown that [SAMs] of dodecane thiol (DDT, 17.6 Å) on Au electrodes are fully blocking (*vide infra* for further comparison with a range of other alkane thiols, Table 2). These data imply the formation of well-organized and virtually pinhole free monolayers of molecules **1** and **2** in a manner similar to that of pure SAMs of DDT. In support of this conclusion, similar profiles were obtained for the cyclic voltammograms for both **1 SAM** and **2 SAM** at different scan rates, i.e. 5, 10, 20, 50 and 100 mV/s. Well-formed monolayers of **2** contacted to gold by the thiol moiety and by the amino functionality prepared using Langmuir-Blodgett techniques reported previously [58] show variable passivation of the electrode surface as a function of the surface pressure used in the deposition step.

The CV response for **3 SAM (Figure 2C)**, showed distinct voltammetric response, with waves similar to those observed in CVs obtained with the bare gold electrode, but with the peak potential shifted to 0.27 V and the currents depressed by 1.39 µA. This suggests macroelectrode behaviour, implying linear diffusion of the redox active species and suggesting that 3 **SAM** has large pinholes in the monolayer. These large defects may be due to the presence of the methoxy side groups which hinder the close packing in the monolayer. **3 SAM** was also investigated at lower scan rates, i.e 10 mV/s and 5 mV/s, and it was observed that there was a very small shift of peak potential (i.e. 0.011 V and 0.001 V) with significant depression in the peak current, i.e. 0.54 µA and 0.41 µA, respectively, compared to the CV at 50mV/s scan rate. Dodecanethiol (DDT) is well known as an excellent candidate for the self-assembly on the gold.[38] Hence mixed SAMs of **3** and DDT were prepared by dipping the substrate in solution containing equal quantities of **3** and DDT (1:1 molar ratio) according to previously published procedures,[39] and the CV response investigated (**Figure 2(C)** dotted line). The mixed 3 SAM and DDT is comparatively pinhole free. However, CV measurements on their own, cannot confirm the existence of mixed SAMs, therefoe, our observations are quantitatively supported by further studies using impedance spectroscopy and

AFM (*vide infra*). CVs of **4 SAM** (**Figure 2(D)**) revealed that the redox reaction is not completely suppressed, exhibiting a sigmoidal shape indicative of microelectrode array behaviour. The voltammogram at a scan rate of 50 mV/s showed a reduction in current by 2.19 µA with no shift in peak potential. When **4 SAM** was investigated at lower scan rates of 10 mV/s and 5 mV/s the current was reduced by a smaller extent, 0.49 µA and 0.25 µA, respectively. As noted above, this behaviour suggests the presence of pinholes and defects in the SAM which are responsible for the diffusion of electroactive species to the gold surface. The strong affinity of both thiol groups for gold resulting in a tendency for alignmentment of the molecular wires **4** parallel to the electrode surface may be the cause of the pinhole type behaviour observed here. The binding of both thiol moieties to the surface results in the collapse of the alignment of the molecular wires leading to the formation of a monolayer with randomly distributed pinholes and defects, consistent with the alignment on the surface proposed by Valkenier et al, for **4**.[43] Further, the CV response of mixed SAMs of **4** and DDT (1:1 molar ratio) was investigated and it was found that although the current was reduced, a clear voltammetric response was still observed, indicating that **4** cannot form a well-organized SAM even when mixed with DDT.

SAMs on Pt electrodes:

The self-assembly of **1, 2, 3** and **4** was further investigated on Pt electrodes. CVs of aqueous solutions of 1 mM $K_4Fe(CN)_6$ solution in 0.1 M KNO_3 between the potential range from -0.2 V to +0.6 V with the scan rate of 50 mV/s are shown in **Figure 2(A'-D')** for both bare Pt working electrodes and Pt working electrodes modified by SAMs of **1**-**4**. The CV of **2 SAM** on Pt shows a sigmoidal scan with a minor shift in peak potential with the current drop by 2.8 µA in comparison to the typical voltammogram of a bare Pt electrode at the scan rate of 50 mV/s.

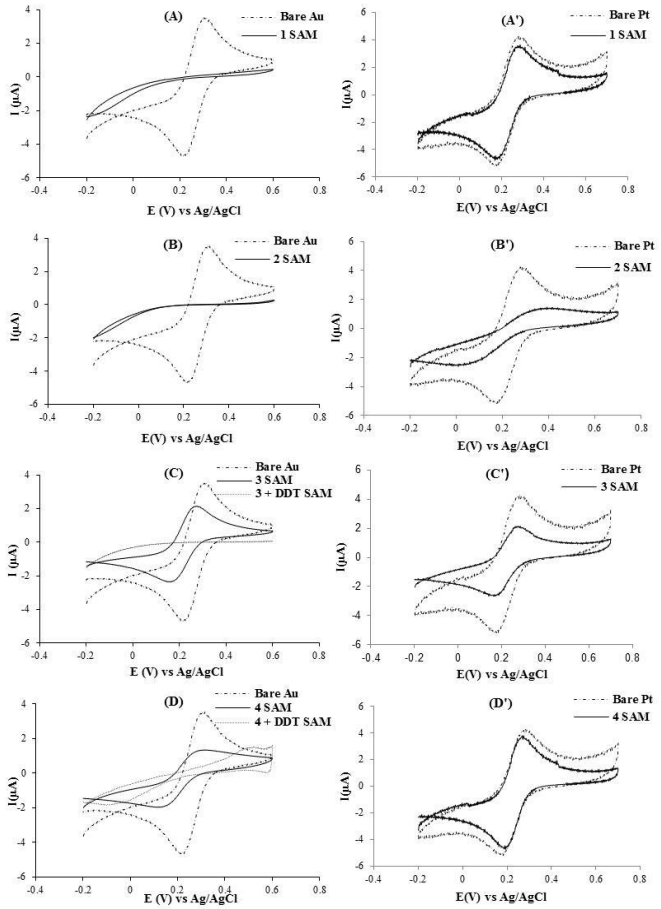

Figure 2. CVs obtained for potential sweep from -0.2V to +0.6V in 1mM $K_4Fe(CN)_6$ + 0.1 M KNO_3 for 1,2 3 and 4 SAMs on Au and Pt electrodes. Scan rate: 50mV s^{-1}.

Further, it was observed that at lower scan rates of 10 mV/s and 5 mV/s, the current drops by only 0.7 µA and 0.3 µA, respectively. Similar CVs were obtained with **3** SAM on a Pt electrode. The CVs at different scan rates leads to the conclusion that the SAMs of **2** and **3** are not of good quality and consist of pinholes and deep defects exist. However, 1 SAMs and **4** SAM on Pt electrode show distinct voltammetric waves, with marginal suppression in current in comparison to the bare Pt electrode which shows the significantly lower coverage of the Pt electrode surface by adsorption of **1** and **4**.

The comparative analysis of the CV study of SAMs of molecular wires **1, 2, 3** and **4** on both metal electrodes leads to the conclusions that the thiol / thioacetate (and amine in the case of **2**) groups do not display a strong affinity for self-assembly on platinum. However, the amine-functionalised molecule **2** shows marginally better affinity for forming SAMs on Pt which may suggest that the competition between amines and thiols for binding to gold is also being observed in the case of **2** on platinum. Furthermore, among the four molecular wires, only **1** and **2** can form well-organised pin-hole free SAMs on gold and are excellent candidates for the self-assembly on gold. Additionally, mono-thiols (e.g. **1**) are better candidates for self-assembly than dithiols (e.g. **4**) which is in good agreement with the results reported by Valkenier et al.[43]

(B) Electrochemical Impedance spectroscopy

Electrochemical impedance spectroscopy (EIS) is a powerful technique for analyzing the quality of SAMs on metal electrodes as it provides quantitative information about the structural integrity of the monolayers. In order to study the SAMs derived from **1-4** on gold and platinum electrodes, EIS measurements were carried out using an AC signal of 10 mV amplitude at the equilibrium potential of the redox couple $Fe(CN)_6^{3-/4-}$ over a wide frequency range from 100 KHz to 1 Hz. The electrolyte solution used was a 1 mM mixture of $Fe(CN)_6^{3-/4}$ solution in 0.1 M KNO_3. EIS measurements were carried out in two parts: (At open circuit potentials, where there is no overpotential at the SAM coated gold electrodes, so that the electron charge transfer due to the defects within the monolayers can be investigated. (b) The DC potential was applied over the range of -0.2 V to +0.6 V (vs. Ag/AgCl) on a SAM coated gold electrode. A semicircle at the high frequency region can be described by a resistance in parallel with constant phase angle capacitor which indicates a kinetically controlled redox reaction and the straight line is described by a Warburg region indicating electron transfer controlled by mass transfer. The Nyquist plots obtained were fitted using equivalent Randles circuit models in the Zplot software supplied with the Solartron 1260.

The apparent electron transfer rate constant K^o_{app} can be obtained by the equation:[42]

$$K^o_{app} = \frac{RT}{n^2F^2cR_{ct}A} \qquad [1]$$

where R is the gas constant, T is temperature, F is the Faraday constant, c is the concentration of the $K_3Fe(CN)_6$ solution, R_{ct} is the charge transfer resistance and A is the geometric area of the electrode. The R_{ct} represents the resistance of the monolayer to the redox species moving through it and was obtained from the fit to the equivalent circuit.

Under equilibrium conditions, the theoretical standard tunnelling rate constant K^o_{th} can be calculated using equation: [42]

$$K^0_{th} = K^0_b \exp(-\beta d) \qquad [2]$$

where, K^o_b is the standard electron transfer rate constant at bare electrode and its value used in this work is 0.031 cm s^{-1}.[61] The parameter β is the exponential decay constant for tunnelling and

measures the magnitude of current lost per unit length of the molecular wire, which can vary from approximately 0 Å^{-1} (metal) to 3.5 Å^{-1} (close to vacuum).[62,63] The β value used in the present work was 0.6033 Å^{-1} and was calculated using value of 0.57 Å^{-1} for each –Ar–C≡C repeat unit and 0.67 Å^{-1} per phenylene group, respectively.[29] The molecular lengths d were calculated using Chem 3D software with MM2 energy minimization potential function. Bond lengths were calculated as the distance of S...C (**1** and **3),** S...N (**2**) and S...S (**4**), bonds.

The fractional coverage of the well-assembled monolayer, θ_a is, estimates the presence of defects in the monolayers and can be calculated using the equation:

$$\theta_a = \frac{\frac{K^0_{app}}{K^0_b} - \exp(-\beta d_o)}{\exp(-\beta d_a) - \exp(-\beta d_0)} \qquad [3]$$

where, d_a represents the average thickness of the whole monolayer (ATWM). An ATWM value close to d_o implies a well-assembled monolayer free from defects.

Nyquist plots of **1-4** SAMs on the gold electrodes in the presence of $Fe(CN)_6^{3-/4-}$ solution at both open circuit and at different potentials versus Ag/AgCl reference electrode were obtained (Figure 3). The experimental and theoretical rate constants of bare electrodes and electrodes coated with **1-4** in 1.0 mM $Fe(CN)_6^{3-/4-}$ + 0.1 M KNO_3 solutions at equilibrium potential were evaluated and the data is summarized in **Table 1**. For the EIS measurements at zero overpotential, the currents predominantly arise by electron tunnelling at defects. Thus, the EIS measurements at zero overpotential give information about the defects and pinholes present in the monolayer. The Nyquist plots of **1** and **2** at zero overpotential showed a large semicircle over the entire range of frequency indicating complete blockage

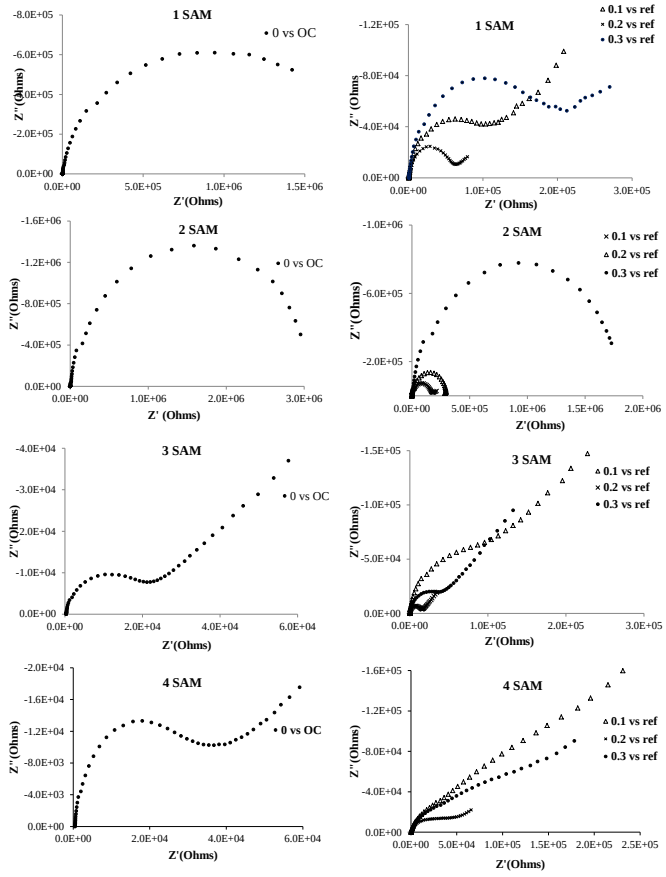

Figure 3. Nyquist plots for Au-SAM electrodes based on molecular wires 1, 2 3 and 4 in 1mM equimolar $K_{3/4}Fe(CN)_6$ + 0.1 M KNO_3 solutions at various potentials. Frequency range: 1 Hz to 100 KHz

of the redox reaction on the electrode surface, characteristic of well-organised and pinhole- and defect-free monolayers. The Nyquist plots of SAMs of **1** and **2**, were fitted with equivalent circuits comprised of a solution resistance (*R1*) in series with a parallel membrane-capacitance related constant phase element (CPE) and a faradaic resistance (*R2*). The R_{ct} values obtained were used to calculate K^o_{th} and K^o_{app} **(Table 1).** It is apparent from the data, K^o_{th} and K^o_{app} values for 1 **SAM 1** and 2 **SAM** on gold surfaces are in good agreement which indicate the formation of well-organised and pin-hole free SAMs.

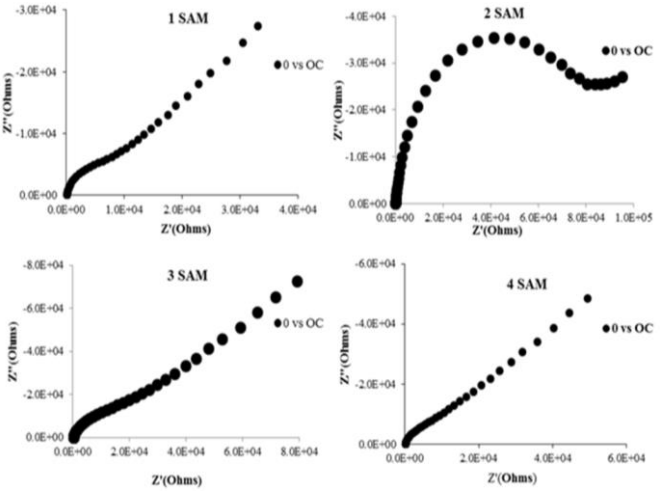

Figure 4. Nyquist plots for Pt-SAM electrodes based on molecular wires 1, 2 3 and 4 in 1mM $K_3Fe(CN)_6$ + 0.1 M KNO_3 solutions in open circuit measurements. Frequency range: 1 Hz to 100 KHz.

Table 1. Experimental and theoretical rate constants of bare electrodes and electrodes coated with thioacetate molecular wires 1, 2, 3 and 4 in 1 mM $K_{3/4}Fe(CN)_6$ + 0.1 M KNO_3 solutions at equilibrium potential

Molecule	Theoretical	$R_{ct\ ocp}$	Experimental
	K^o_{th} (cm s^{-1})	(KΩ)	K^o_{app} (cm s^{-1})
	Gold SAMs		
1	2.525E-07	1.46E06	6.66E-07
2	2.030E-07	3.05E06	4.21E-07
3	2.525E-07	1.78E04	7.44E-05
3+DDT	-	3.31E07	4.02E-08
4	1.641E-07	6.03E04	2.20E-05
4+DDT	-	2.85E05	4.66E-06
	Platinum SAMs		
1	2.525E-07	7.57E03	1.12E-04
2	2.030E-07	7.51E04	1.13E-05
3	2.525E-07	1.39E04	60.08E-05
4	1.641E-07	2.66E03	3.18E-04

The marginal difference in theoretical and experimental electron transfer rate constants can be attributed to minor defects and small tunnelling currents in the monolayers of **1** and **2**. The Nyquist curves at various potentials versus Ag/AgCl reference electrode show evidence of mass charge transport with an increase in positive potentials.

The Nyquist plots of **3** and **4** SAMs of on gold electrode showed a semicircle at the high frequency region and a straight line at the low frequency region, indicating the existence of kinetically controlled charge transport characteristic of facile charge transfer and consequently an uneven poor quality SAMs on the electrode surface. Furthermore, the difference of order of 10^2 in the values

of K^{o}_{th} and K^{o}_{app} for both SAMs of **3** and **4** corroborate the CV studies which also indicate the poor blocking behaviour of these SAMs.

EIS measurements were carried out, in a similar manner, on **1, 2, 3** and **4** SAMson a platinum electrode using an AC signal of 10 mV amplitude at the equilibrium potential of the redox couple $Fe(CN)_6^{3-/4-}$ over a wide frequency range from 100 KHz to 1 Hz. The electrolyte solution used was 1 mM $Fe(CN)_6^{3-/4-}$ solution in 0.1 M KNO_3. The Nyquist plots at zero overpotential (**Figure 4**) indicate that only **2** and **3** self- assemble on the platinum electrode to partially, in comparison to the molecules **1** and **4**. This is further confirmed by analyzing the differences in the values of the theoretical and experimental electron transfer rate constants.The influence of K^{o}_{app} **(Table 1)** on the nature of the blocking properties of the SAM of molecules **1-4** can be obtained by using eqn (3) **(Figure 5)** by plottting the values of θ_a versus d_a for SAMs of molecular wires **1-4** on both gold and platinum electrodes. Both, **1** and **2** form good quality SAMs on gold with an average thickness of 18 Å and 18.6 Å, respectively. On other hand, for **3** and **4,** the values of ATWM are only 10 Å and 12.1 Å which suggests the presence of pinholes and defects in their respective monolayers on gold. In comparison to the SAMs on gold electrodes, the maximum average thickness of **1, 2, 3** and **4** on the platinum electrode are 9.4 Å, 13.2 Å, 10.4 Å and 7.6 Å, respectively, which suggest that all the SAMs have deep defects and are far from the ideal ATWM values.

The results of the EIS study agree very well with those obtained from the CV study confirming that **1** and **2** are excellent candidates for self-assembly on gold, in comparison to **3** and **4**. However, none of the four molecules forms a good quality SAM on Pt electrodes.

Finally, the apparent electron transfer rate constants through the SAMs of **1** and **2** on gold electrodes were analyzed in comparison to the electron transfer rates through self-assembled monolayers of a range of alkane thiols previously reported in the literature (**Table 2**). It can be seen that the SAMs of **1** and **2** have better blocking capacity in comparison to short alkanethiols such as heptanethiol and nonanethiol as well as dodecanethiol which is one of the best candidates for self-assembly on gold. The rate constants of SAMs of **1** and **2** are in good agreement with those reported for the long-chain hexadecanethiol.

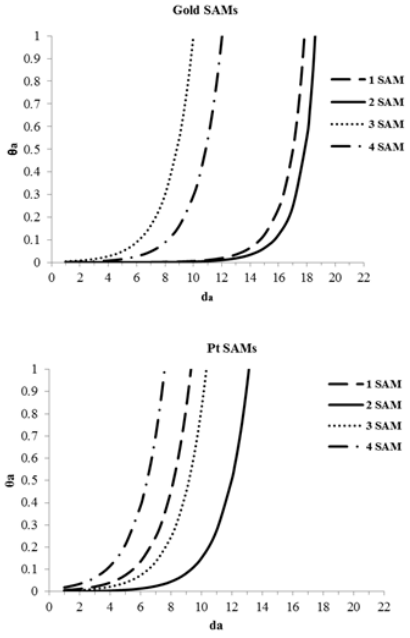

Figure 5. θ_a vs. d_a plots of SAMs of 1, 2, 3 and 4 on gold and platinum electrodes.

Table 2: Comparison studies of experimental rate constant of self-assembled monolayers previously reported in literature

Experimental

Molecule	K^{o}_{app} (cm s^{-1})	Reference
1	6.66E-07	Present work
2	4.21E-07	Present work
1-Heptanethiol	2.59E-03	Ref. 42
Nonanethiol	9.21E-05	Ref. 64
Dodecanethiol	1.08E-06	Ref. 64
Hexadecanethiol	1.44E-07	Ref. 64
Octadecanethiol	3.28E-08	Ref. 64
Octadecanethiol	2.90E-07	Ref. 28
Oligo(aryleneethylene)	6.61E-05	Ref. 42

Morphology and structural studies

(A) Atomic Force Microscopy (AFM)

Atomic force spectroscopy (AFM) was used to analyze the structural features of SAMs. The SAMs derived from **1-4** on gold were imaged using AFM in tapping mode (**Figure 6)** showing the 3D images and AFM section analyses of four SAMs. The section analysis of the height images gave root-mean-square (RMS) roughness of 0.607 nm for the bare gold and 2.671 nm, 2.825 nm, 1.017 nm and 1.414 nm for SAMs of **1, 2, 3** and **4** respectively. It can be clearly seen (**Figure 6**) that **1** and **2** form dense, well packed monolayers with maximum surface coverage. The surface roughness of the SAM of **3** is approximately 0.4 nm greater than that of the bare gold surface which suggests minimal and partial surface coverage of SAM formed by this molecule. The roughness factor with the SAM of **4** is more than that of the bare gold which suggests formation of a layer. However, in comparison to the SAMs of **1** and **2**, the RMS value for **4** is much less which suggests that molecules of **4** may be collapsed on the surface due to binding from both ends of the molecule.

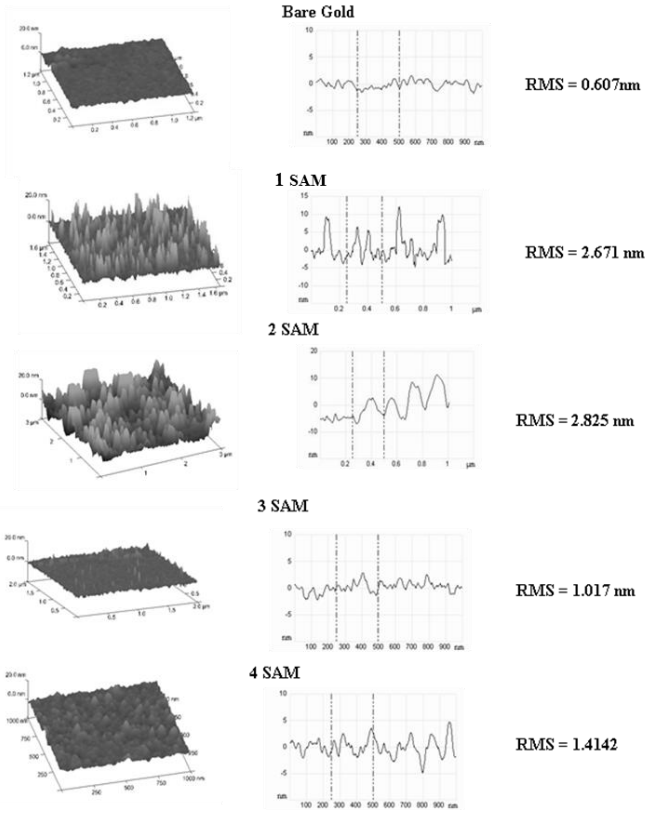

Figure 6. AFM 3D images and section analysis of SAMs of **1**, **2**, **3** and **4** on gold electrodes.

The AFM data are, therefore, entirely consistent with the results obtained from CV and EIS studies.

No AFM imaging was performed for SAMs on platinum. as it was concluded on the basis of CV and EIS studies that none of the four molecules form well-organised monolayers on the platinum electrode surface.

Conclusion

SAMs derived from four bifunctional molecules **1, 2, 3** and **4** on gold electrodes have been thoroughly studied using techniques: CV, EIS and AFM. It has been clearly shown that **1** and **2** behave as rigid rod molecular wires suitable for self-assembly on a gold surface and form well-ordered, dense monolayers with S-Au bonds. SAMs of **3** show pin-hole behaviour even in mixed monolayers with dodecanethiol (DDT), due to the steric hindrance of the methoxy side chains. SAMs of dithioacetate **4**, indicate binding from both ends to the gold surface which does not allow dense packing and leads to the formation of monolayers with randomly distributed pinholes. Further, it can be concluded that none of the four molecular wires studied can act as a suitable candidate for the self-assembly on a platinum electrode. This work should provide further impetus to explore SAMs of new OPEs as key structural elements for a range of nanotechnology applications.

Experimental Section

Materials: Compounds **1, 4**, potassium ferrocyanide, 1-dodecanethiol (DDT), were purchased from Sigma-Aldrich and were used as received. Potassium nitrate was purchased from Lancaster. Tetrahydrofuran (THF), hydrogen peroxide and sulfuric acids were purchased from Acros Organics and Fluka, respectively. All solvents were purified by suitable methods and all aqueous solutions were prepared using deionized water obtained from Sartorius Arium 611 ultrapure water system (conductivity = 0.055 μS cm^{-1}). Polycrystalline gold and platinum disc electrodes with the diameter of 1.6 mm and 2.0 mm, respectively, were used for the preparation of self-assembled monolayers. Thioacetates **2**[58] and **3**[60] were synthesized as reported previously.

Preparation of self-assembled monolayers: Prior to use of the electrodes for SAM deposition, the electrodes were thoroughly cleaned by polishing for 2 min in a figure-eight pattern on Buhler Microcloth, sequentially with diamond polish slurries of 15, 6, 3 and 1 μm followed by sonication in ethanol and water.[65,66] Cyclic voltammetry in 1 M H_2SO_4 solution from 0 V to 1.5 V (vs. Ag/AgCl/KCl, 3.5 M) was employed as a measure of the cleanliness of the gold electrode surface. If required, the gold electrodes were also cleaned by soaking in Piranha solution for a few minutes, followed by rinsing with water. The typical shape of the voltammogram and charge under the stripping wave larger than 1.4 μC cm^{-2} served as a measure of cleanliness of the electrode. After sonication in water and ethanol, the gold electrodes were dried under a stream of argon and were ready for the deposition of self-assembled monolayers. The Pt electrodes were cleaned similarly and the cleanliness of the surface was verified by CV in 0.5 M H_2SO_4 in the potential range from -0.2 V to 1.2 V. SAMs were deposited on the Au and Pt electrodes by immersing the clean electrodes in 1.0 mM in THF solution of **1, 2, 3** and **4** for 24 h at room temperature. Loosely bound molecules were removed by rinsing with THF and the electrodes were then dried with a slow stream of argon.

Instruments: A Potentiostat-Galvanostat Model 283 (Princeton Applied Research) was used for cyclic voltammetric studies and CVs were run by sweeping the potentials from -0.2 V to +0.6 V. The electrochemical impedance spectroscopy (EIS) measurements were carried out using a Solarton 1260 Impedance/Gain-Phase Analyser connected with a PAR model 283 potentiostat interfaced with a personal computer. In EIS, sinusoidal potential sweeps with the frequencies varying from 0.1 Hz to 100 KHz are applied to the Au or Pt electrode. The Zplot software supplied with the Solartron 1260 was used to collect, plot and interpret the raw impedance data. A three electrode cell was employed in all experiments. The reference electrode used was Ag/AgCl (3.5 mol dm^{-3} KCl). A Pt foil (A = 1 cm^2) was used as counter electrode. Bare gold/Pt electrode or electrodes covered with SAMs acted as the working electrode. The cell was placed in a Faraday cage to isolate the system from the external inference. All potentials are reported with respect to Ag/AgCl (3.5 mol dm^{-3} KCl). All measurements were carried out at room temperature in the solutions purged of oxygen by bubbling argon for 10 min. The Nyquist plots were fitted using equivalent Randles circuit models.

Atomic force microscopy (AFM) was applied to examine the roughness of surface of the monolayers. AFM height images were obtained using Nanoscope 4 multimode Digital AFM (Veeco Instruments, Inc.) in tapping mode. Gold substrates were prepared on glass by evaporation of an adhesion layer of 10 nm chromium and 200 nm gold, respectively. Subsequently, the substrate was immersed into a 1 mM adsorbate solution in THF. AFM investigations confirmed the flatness of the surface. The gold substrate bearing self-assembled monolayers were glued to the steel disk on top of an XYZ translator. The AFM tip was positioned close to the surface and samples were scanned in the tapping mode.

Acknowledgements

The authors acknowledge the financial support from the Department of Science and Technology, India and Durham University for providing research facilities. X.Z. thanks the China Scholarship Council for the award of a scholarship. RK thanks Dr Paula Lopes with help in formatting the manuscript.

Keywords: Self-assembly, monolayers, Impedance, Cyclic voltammetry, Oligo(phenyleneethynylene), Fractional coverage, gold, platinum

References:

[1] D. Mandler, I. Turyan, *Electroanalysis* **1996**, *3*, 207-213.
[2] I. Turyan, D. Mandler, *Anal. Chem.* **1997**, *69*, 894-897.
[3] X. -H. Zhang, S. -F. Wang, *Anal. Lett.* **2002**, *35*, 995-1006.
[4] M. Hepel, J. Dallas, *Sensors* **2008**, *8*, 7224-7240.
[5] A. Veselov, C. Thür, A. Efimov, M. Guina, H. Lemmetyinen, N. Tkachenko, *Meas. Sci. Technol.* **2010**, *21*, 115205-115214.
[6] J. -Y. Park, Y. -S. Lee, B. -Y. Chang, B .H. Kim, S. Jeon, S. -M. Park, *Anal. Chem.* **2010**, *82*, 8342-8348.
[7] I. Marques de Oliveira, F. Vocanson, J. Uttaro, Z. Asfari, C.A. Mills, J. Samitier, A. Errachid, *J Nanosci. Nanotechnol.* **2010**, *10*, 413-420.
[8] N. K. Chaki, K. Vijyamohan, *Biosens. Bioelectron.* **2002**, *17*, 1-12.
[9] K. Haupt, K. Mosbach, *Chem. Rev.* **2000**, *100*, 2495-2504.
[10] B. L. Hassler, R. M. Worden, *Biosens. Bioelectron.* **2006**, *21*, 2146-2154.
[11] A. Fragoso, N. Laboria, D. Latta, C. K. O'Sullivan, *Anal. Chem*. **2008**, *80*, 2556-2563.
[12] C. Silien, M. Buck, G. Goretzki, D. Lahaye, N. R. Champness, T. Weidner, M. Zharnikov, *Langmuir* **2009**, *25*, 959-967.
[13] S. K. Arya, P. R. Solanki, M. Datta, B. D. Malhotra, *Biosens. Bioelectron.* **2009**, *24*, 2810-2817.
[14] Y. Wang, Y. Zhou, J. Sokolov, B. Rigas, K. Levon, M. Rafailovich, *Biosens. Bioelectron.* **2008**, *24*, 162-166.
[15] H. Chen, C. K. Heng, P. D. Puiu, X. D Zhou, A. C. Lee, T. M. Lim, S. N. Tan, *Anal. Chim. Acta* **2005**, *554*, 52-59.
[16] T. J. Huang, B. Brough, C.-M. Ho, Y. Liu, A. H. Flood, P. A. Bonvallet, H.-R. Tseng, J. F. Stoddart, M. Baller, S. Magonov, *Appl. Phys. Lett.* **2004**, *85*, 5391-5393.
[17] O. Azzaroni, M.Cipollone, M. E. Vela, R. C. Salvarezza, *Langmuir* **2001**, *17*, 1483-1487.
[18] G. Brunoro, A. Frignani, A. Colledan, C. Chiavari, *Corros. Sci.* **2003**, *45*, 2219-2231.
[19] C. M. Whelan, M. Kinsella, L.Carbonell, K. Maex, *Microelectron. Eng.* **2003**, *70*, 551-557.
[20] J. M. Tour, *Acc. Chem. Res.* **2000**, *33*, 791-804.
[21] T. Sugawara, M. M. Matsushita, *J. Mater. Chem.* **2009**, *19*, 1738-1753.
[22] A. Lio, D. H. Charych, M. Salmeron, *J. Phys. Chem. B* **1997**, *101*, 3800-3805.
[23] P. E. Sheehan, L. J. Whitman, *Phys. Rev. Lett.* **2002**, *88*, 156104-156107.
[24] J. A. Helmuth, H. Schmid, R. Stutz, A. Stemmer, H. Wolf, *J. Am. Chem. Soc.* **2006**, *128*, 9296-9297.
[25] J. M. McLellan, M. Geissler, Y. Xia, *J. Am. Chem. Soc.* **2004**, *126*, 10830-10831.
[26] A. A. Dameron, J. R. Hampton, R. K. Smith, T.J. Mullen, S. D. Gillmor, P. S. Weiss, *Nano Lett.* **2005**, *5*, 1834-1837.
[27] C. -J. Zhong, J. Zak, M. D. Porter, *J. Electroanal. Chem.* **1997**, *421*, 9-13.
[28] P. Diao, M. Guo, D. Jiang, Z. Jia, X. Cui, D. Gu, R. Tong, B. Zhong, *J. Electroanal. Chem*. **2000**, *480*, 59-63.
[29] M. A. Rampi, G. M. Whitesides, *Chem. Phys*. **2002**, *281*, 373-391.
[30] R. Brito, R. Tremont, C. R. Cab*rera, J. Elec**tro**anal. Chem.* **2004**, *574*, 15-22.

[31] B. I. Rosario-Castro, E. *R. Fachini, J. Hernández*, *M.* E. Pérez-Davis, C. R. Cabrera, *Langmuir* **2006**, *22*, 6102-6108.
[32] P. Diao, D. Jiang, X. Cui, D. Gu, R. Tong, B. Zhong, *J. Electroanal. Chem*. **1999**, *464*, 61-67.
[33] T. Kawaguchi, H. Yasuda, K. Shimazu, M. D. Porter, *Langmuir* **2000**, *16*, 9830-9840.
[34] S. A. John, F. Kitamura, K. Tokuda, T. Ohsaka, *Langmuir* **2000**, *16*, 876-880.
[35] P. Diao, M. Guo, R. Tong, *J. Electroanal. Chem*. **2001**, *495*, 98-105.
[36] X. Xiao, B. Wang, C. Zhang, Z. Yang, M. M. T. Loy, *Surf. Sci.* **2001**, *472*, 41-50.
[37] O. Azzaroni, M. E. Vela, H. Martin, A. Hernandez Creus, G. Andreasen, R. C. Salvarezza, *Langmuir* **2001**, *17*, 6647-6654.
[38] Y. F. Xing, S. J. O'Shea, S. F. Y. Li, *J. Electroanal. Chem*. **2003**, *542*, 7-11.
[39] H. Ye, R. W. J. Scott, R. M. Crooks, *Langmuir* **2004**, *20*, 2915-2920.
[40] S. S. Datwani, R. A. Vijayendran, E. Johnson, S. A. Biondi, L*angmuir* **2004**, *20*, 4970-4976.
[41] C. Vericat, M. E. Vela, G. Benitez, P. Carro, R. C. Salvarezza, *Chem. Soc. Rev.* **2010**, *39*, 1805-1834.
[42] F. A. Aguiar, R. Campos, C. Wang, R. Jitchati, A. S. Batsanov, M. R. Bryce, R. Kataky, *Phys. Chem. Chem. Phys.* **2010**, *12*, 14804-14811.
[43] H. Valkenier, E. H. Huisman, P. A. van Hal, D. M. de Leeuw, R. C. Chiechi, J. C. Hummelen, *J. Am. Chem. Soc.* **2011**, *133*, 4930-4939.
[44] J. Clavilier, V. Svetličić, V. Žutić, *J. Electroanal. Chem*. **1996**, *402*, 129-135.
[45] R. Brito, V.A. Rodríguez, J. Figueroa, C. R. Cabrera, *J. Electroanal. Chem.* **2002**, *520*, 47-52.
[46] R. Brito, R. Tremont, O. Feliciano, C. R. Cabrera, *J. Electroanal. Chem.* **2003**, *540*, 53-59.
[47] R. Tremont, H. De Jesús-Cardona, J. García-Orozco, R. J. Castro, C. R. Cabrera, *J. Appl. Electrochem.* **2000**, *30*, 737-743.
[48] R. Tremont, C. R. Cabrera, *J. Appl. Electrochem.* **2002**, *32*, 783-793.
[49] S. W. Han, S. J. Lee, K. Kim, *Langmuir* **2001**, *17*, 6981-6987.
[50] S. L. Brandow, M. S. Chen, R. Aggarwal, C. S. Dulcey, J. M. Calvert, W. J. Dressick, *Langmuir* **1999**, *15*, 5429-5432.
[51] Z. Q. Wei, C. Wang, C. F. Zhu, C.Q. Zhou, B. Xu, C. L. Bai, *Surf. Sci.* **2000**, *459*, 401-412.
[52] M. D. Porter, T. B. Bright, D. L. Allara, C. E. D. Chidsey, *J. Am. Chem. Soc.* **1987**, *109*, 3559-3568.
[53] H. O. Finklea, S. Avery, M. Lynch, T. Furtsch, *Langmuir* **1987**, *3*, 409-413.
[54] E. Sabatani, I. Rubinstein, R. Maoz, J. Sagiv, *J. Electroanal. Chem.* **1987**, *219*, 365-371.
[55] N. Weibel, S. Grunder, M. Mayor, *Org. Biomol. Chem*. **2007**, *5*, 2343-2353.
[56] A. Beeby, K. Findlay, P.J. Low, T. B. Marder, *J. Am. Chem. Soc.* **2002** *124*, 8280-8284.
[57] S. J. Greaves, E. L. Flynn, E. L. Futcher, E. Wrede, D. P. Lydon, P. J. Low, S. R. Rutter, A. Beeby, *J. Phys. Chem. A* **2006**, *110*, 2114-2121.
[58] L. M. Ballesteros, S. Martín, G. Pera, P. A. Schauer, N. J. Kay, M. C. López, P. J. Low, R. J. Nichols, P. Cea, *Langmuir*, **2011**, *27*, 3600-3610.
[59] G. J. Ashwell, A. T. Williams, S. A. Barnes, S. L. Chappel, L. J. Phillips, B. J. Robinson, B. Urasinska-Wojcik, P. Wierzchowiec, I. R. Gentle, B. J. Wood, J. Phys. Chem. C 2011, 115, 4200-4208.
[60] S. Martín, I. Grace, M. R. Bryce, C. Wang, R. Jitchati, A. S. Batsanov, S. J. Higgins, C. J. Lambert, R. J. Nichols, *J. Am. Chem. Soc*. **2010**, *132*, 9157-9164.
[61] V. Marecek, Z. Samec, J. Weber, *J. Electroanal. Chem.* **1978**, *94*, 169.
[62] P. P. Edwards, H. B. Gray, M. T. J. Lodge, R. J. P. Williams, *Angew. Chem., Int. Ed.* **2008**, *47*, 6758-6765.
[63] D. K. James, J. M. Tour, *Chem. Mater.* **2004**, *16*, 4423-4435.
[64] L. V. Protsailo, W. R. Fawcett, *Electrochimica Acta* **2000**, *45*, 3497-3505.
[65] H. O. Finklea, Encyclopedia of Analytical Chemistry; R. A. Meyers, Ed.; John Wiley & Sons, Ltd: Chichester, UK., 2000.
[66] D. L. Allara, R. G. Nuzzo, Langmuir, 1985, 1, 45.

Received: ((will be filled in by the editorial staff))
Published online: ((will be filled in by the editorial staff))

Entry for the Table of Contents

ARTICLES

Thiol terminated rigid rod wire like oligo (phenyleneethynylene)s assembled on electrodes show charge transfer properties which are dependent on their structure and terminal group.

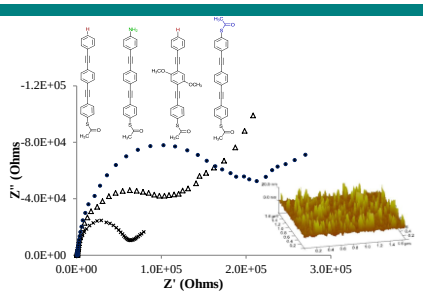

(Inderpreet Kaur, Xiaotao Zhao, Martin R. Bryce, Phil A. Schauer, Paul J. Low and Ritu Kataky)*

Page No. – Page No.

Modification of electrode surfaces by self-assembled monolayers of thiol-terminated oligo(phenyleneethynylene)s